HOKKAIDO UNIVERSITY

Title	Neural Network for Both Metal Object Detection and Coil Misalignment Prediction in Wireless Power Transfer
Author(s)	Gong, Yunyi; Otomo, Yoshitsugu; Igarashi, Hajime
Citation	IEEE Transactions on Magnetics, 58(9), 7201004 https://doi.org/10.1109/TMAG.2022.3176908
Issue Date	2022-09
Doc URL	https://hdl.handle.net/2115/86618
Rights	© 2022 IEEE. Personal use of this material is permitted. Permission from IEEE must be obtained for all other uses, in any current or future media, including reprinting/republishing this material for advertising or promotional purposes, creating new collective works, for resale or redistribution to servers or lists, or reuse of any copyrighted component of this work in other works.
Type	journal article
File Information	TMAG_Gong-publish1.pdf

Hokkaido University Collection of Scholarly and Academic Papers : HUSCAP

Neural Network for Both Metal Object Detection and Coil Misalignment Prediction in Wireless Power Transfer

Yunyi Gong[1], Yoshitsugu Otomo[2], and Hajime Igarashi [1], *Member, IEEE*

[1] Graduate School of Information Science and Technology, Hokkaido University, Sapporo, 060-0814, Japan
[2] Graduate School of Engineering, Nagasaki University, Nagasaki, 852-8521, Japan

This study proposes a method for wireless power transfer systems to identify the existence of foreign metal objects and simultaneously predict the misalignment distance between the primary and secondary coils. The proposed method is based on a neural network (NN) trained using electromagnetic field simulations. The training data for the NN consist of the differential voltages in the detection coils, together with the input voltage of the primary coil. Although the metallic objects and coil misalignment induce confusing voltages, the trained NN exhibits over 90% accuracy for the validation dataset, and mean prediction errors of less than 1 mm for the misalignment distance and ground clearance variance.

***Index Terms*— Wireless power transmission, Object detection, Neural networks.**

I. Introduction

Recently, the attention paid to electric vehicles (EVs) has been increasing due to environmental concerns about global warming. This has promoted the intensive study of wireless power transfer (WPT), which allows reliable charging of EVs. Until now, many studies on the design of coils and magnetic cores for WPT have been performed with the goal of increasing transfer efficiency [1]-[2].

In addition to performance, safety is an important consideration for WPT. Many studies have focused on reducing the leakage flux of WPT [3] to mitigate the magnetic flux exposure to human bodies, the safe limit for which is stipulated by ICNIRP as 27 μT for frequency bands ranging from 3 kHz to 10 MHz [4].

Another possible risk for WPT systems is caused by foreign metal objects, which may lead to dangerous electric discharge and fire accidents when exposed in the strong alternative magnetic field of a WPT system. For this reason, metal object detection (MOD) has been studied. Differential voltage coils [5]-[6] have been introduced to detect the voltage induced by a metal object. However, detection coils might not work well when there is misalignment in the primary and secondary coils, which generates confusing voltages. MOD without additional sensors or detection coils has also been proposed [7]-[8], but the validity of this approach is unclear when magnetic cores are introduced to a WPT system, because an increase in the magnetic flux complicates the field distribution. Robust and accurate MOD is required that will work effectively even if confusing voltages are generated owing to coil misalignment or magnetic cores.

Moreover, misalignment between the transmitting coils also influences the performance of WPT systems, including the transfer efficiency and leakage magnetic field. In [9], the misalignment was predicted from the voltage induced in the sensor coils near the winding on the primary coil, where the extreme gradient boost algorithm was employed for the prediction. Similar sensor coils were used for MOD [10].

In summary, coil misalignment and metal object can be threat to the performance and safety of WPT system. It would become worse when the two problems coexist. However, it is unclear whether MOD and prediction of the misalignment distance can be performed simultaneously. If this is possible, the performance and safety of WPT can be improved significantly.

In this study, we propose a method based on a neural network (NN) that simultaneously performs MOD and prediction of the misalignment and clearance variance in the WPT system. We train the NN using repeated electromagnetic field simulations, though it can also be trained using measured data.

II. Simulation Model

A WPT system driven by a 1 A current source was considered in the analysis. The capacitors were connected to the primary and secondary coils in series, and the capacitance was adjusted so that the WPT system had resonance at 85 kHz. The load of the system is assumed to be a 20 Ω resistor connected to the secondary coil.

The WPT device consists of the transfer coils as shown in Fig. 1, in which we arrange bar-shaped magnetic cores with a design according to [11], with a relative permeability of 3300, to increase the coupling between the primary and secondary coils. The transfer coils have 15 and 10 turns of coils, 4.5 mm in diameter, as shown in Fig. 2, where r_{in} and r_{out} which denote the inner and outer radius of coils are 77.5 and 145 mm for 15 turns, while they are 100 and 145 mm for 10 turns. The self-inductances are approximately 86.9 μH and 52.1 μH. We verified the proposed method using these different models.

Manuscript received April 1, 2015; revised May 15, 2015 and June 1, 2015; accepted July 1, 2015. Date of publication July 10, 2015; date of current version July 31, 2015. (Dates will be inserted by IEEE; "published" is the date the accepted preprint is posted on IEEE Xplore®; "current version" is the date the typeset version is posted on Xplore®). Corresponding author: Y. Gong (e-mail: gongyunyi@em.ist.hokudai.ac.jp).

Color versions of one or more of the figures in this paper are available online at http://ieeexplore.ieee.org.

Digital Object Identifier (inserted by IEEE).

0018-9464 © 2015 IEEE. Personal use is permitted, but republication/redistribution requires IEEE permission.
See http://www.ieee.org/publications_standards/publications/rights/index.html for more information. (Inserted by IEEE.)

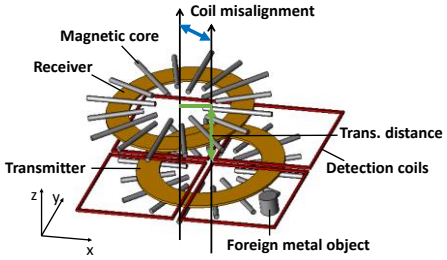
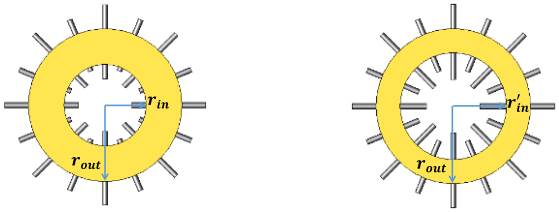


Fig. 1. WPT model.



(a) 15 turns (L ≈ 86.9 μH) (b) 10 turns (L ≈ 52.1 μH)

Fig. 2. Primary coil.

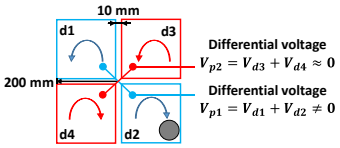


Fig. 3. Differential coils.

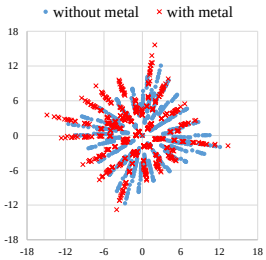
Four one-turn square detection coils were placed on the transmitter. The diagonal coil pairs, $p_1(d1, d2)$ and $p_2(d3, d4)$, are wound in opposite directions to detect the differential voltage. The concept of differential voltage is simple. For example, as shown in Fig. 3, when a metal object is placed above coil $d2$, the induced voltages of $p_1(d1, d2)$ cannot be canceled and the differential voltage will not be zero, while that of $p_2(d3, d4)$ is still zero. Therefore, the existence of metal objects can be recognized. The misalignment in the two coils causes confusing voltages in the detection coils. In this study, we predict the existence of metals and the misalignment distance from the detected signals, which would be difficult for humans because of the complexity and high dimensionality of the signals.

Neglecting the fine wire structures, we assume pancake-shaped coils for WPT with a uniform current of 1 A. An aluminum cylinder with a diameter of 35 mm and height of 35 mm is assumed as the foreign metal object. This object has similar or smaller size in comparison with a can and bar listed in IEC 61980-3 [12]. The eddy current in the aluminum cylinder is considered in the field computation using JMAG®.

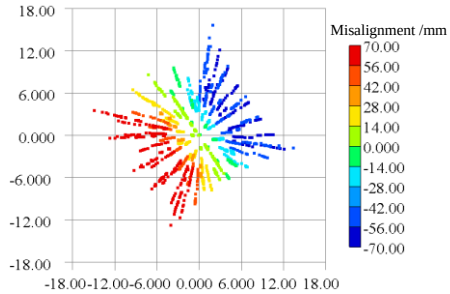
III. Proposed Method Based on NN

A. Data preparation

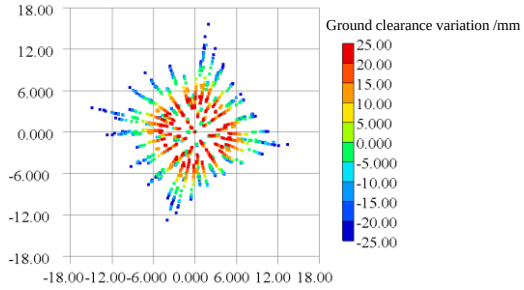
We assume that the distance between the primal and secondary coils ranges from 50 to 100 mm, namely the distance assumed to be 75 ±25 mm, while the coil misalignment on the *x-y* plane ranges from -70 to 70 mm. The metal object is assumed to have a random position within the space covered by the detection coils.



(a) marked according to the existence of a metal object



(b) marked according to misalignment in the x direction



(c) marked according to variance on clearance in z direction

Fig. 4. Visualization of $\{V_p\}$ through SVD

In total we built 1500 cases, half with and half without a foreign metal object. For each case, we computed and stored the differential voltages of the detection coil pairs and the input voltage of the primary coil at 85 kHz.

From these data, we constructed two vectors

$$\boldsymbol{V}_{in} = [u_1^r, u_1^i, u_2^r, u_2^i, \dots] \quad (1)$$

$$\boldsymbol{V}_p = [v_{11}^r, v_{11}^i, v_{12}^r, v_{12}^i, v_{21}^r, v_{21}^i, v_{22}^r, v_{22}^i, \dots] \quad (2)$$

where the quantities with indexes *r* and *i* denote the real and imaginary components, $\boldsymbol{V}_{in}$ is composed of the input voltages $u_k = u_k^r + ju_k^i$ of the primary coil, while $\boldsymbol{V}_p$ consists of the differential voltages $v_{kl} = v_{kl}^r + jv_{kl}^i$ of the *l*-th pair for the cases $k = 1,2, \dots$.

To understand the data properties, the vectors $\boldsymbol{V}_p$ for the 15 turns model are mapped on the two-dimensional plane by singular value decomposition (SVD) as shown in Fig. 4. Fig. 4 (a) shows the distribution of cases with and without the metal object, where a point corresponds to a case. Fig. 4 (b) and (c) show the distribution of the data with different misalignment distances in the *x* direction, and clearance variation in *z* direction, respectively. The figures show a clear correlation between the misalignment and variation, but not for the existence of metal objects, at least in the two-dimensional plane.

B. Neural network

We implemented an NN using Tensorflow® [13] and Python. The hyperparameters are listed in Table I, and the structure of

the NN is shown in Fig. 5. The input data are either $\{\boldsymbol{V}_{in}, \boldsymbol{V}_p\}$ or $\{\boldsymbol{V}_p\}$, which are standardized before being provided to the NN. We configured four dense layers composed of 64 neurons whose activation function was set to ReLU. The NN has four outputs representing the existence possibility of the metal object, the misalignment distances and the clearance variance in z direciton. The loss functions and weighting coefficients for the losses are included in Table I.

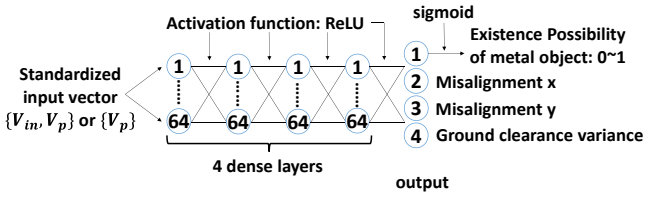


Fig. 5. NN structure.

TABLE I
HYPERPARAMETERS OF THE NN

Batch size	20
Epochs	750
Optimizer	Adam
Learning rate	0.001
Loss function (MOD)	Binary cross entropy
Loss function (position prediction)	Huber loss
Loss weights (MOD : position prediction)	1 : 0.01

IV. TRAINING AND VALIDATION

A. *K-fold cross validation*

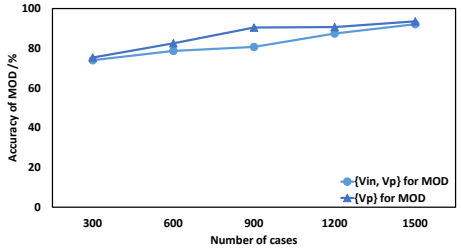
To evaluate the prediction accuracy, 5-fold cross validation was applied to NNs for the 15-turn model, which was trained using either the combined data $\{\boldsymbol{V}_{in}, \boldsymbol{V}_p\}$ or $\boldsymbol{V}_p$. All the data were divided into five subsets, and the NN was trained five times, with four subsets used for training while the remaining subset was used for the validation of prediction accuracy. The average performance over the five training sessions was treated as the final performance of the NN. K-fold cross-validation was implemented using Scikit-learn® [14]. The same procedure was applied to the 10-turn model.

B. *Training results*

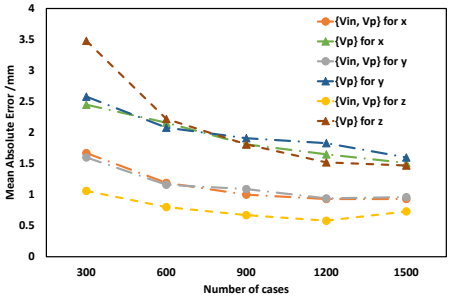
The performance of the trained NNs is shown in Table II, which includes the accuracy of MOD and the mean absolute error in the prediction of misalignment distances (Error in x, y) and clearance variance (Error in z). For both result types, the accuracy of the 15-turn model is better than that of the 10-turn model. The accuracy of MOD for the former model is over 90% for both cases based on $\{\boldsymbol{V}_{in}, \boldsymbol{V}_p\}$ and $\boldsymbol{V}_p$ while that for the latter is between 80% and 85%. This is because the 15-turn model has a larger inductance, so that a larger magnetic field is generated between the coils, causing a larger eddy current loss in the metal object. This results in a larger change in $\boldsymbol{V}_{in}$ and $\boldsymbol{V}_p$ caused by the metal object. For this reason, MOD becomes easier.

The prediction accuracy for the misalignment distance and clearance variance was clearly improved by adding $\boldsymbol{V}_{in}$ to the input data. This tendency is more remarkable in the 10-turn model; the prediction error is reduced to less than 20% by using $\boldsymbol{V}_{in}$ in addition to $\boldsymbol{V}_p$. These results suggest that the use of $\{\boldsymbol{V}_{in}, \boldsymbol{V}_p\}$ as the input data is preferable for our purpose. It is noted that the predicted misalignment and clearance variance error in z direction can be sent to the user of the WPT, who can make a fine alignment to improve the energy transfer efficiency.

Next, we consider the dependence of performance on the amount of data. We randomly thin the data to create new data sets with sizes ranging from 300 to 1500 cases. NNs were trained and evaluated using the different numbers of cases. Fig. 6 shows the dependence of the performance of the trained NN for the 15-turn model on the number of cases. The accuracy of the MOD increases, and the prediction error in the alignment distance decreases, with the number of cases. A similar tendency was observed for the 10-turn model.



(a) Accuracy of MOD



(b) prediction error in the x, y misalignment, and clearance variation in z.

Fig. 6. Dependence of performance on number of cases for the 15-turn model

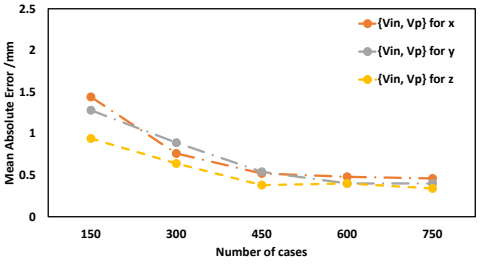


Fig. 7. Dependence of misalignment distance error in the x, y, and clearance variation in z on the number of cases (15turns, without MOD).

TABLE II
MOD ACCURACY AND ERROR IN POSITION PREDICTION OF TRAINED NN

	15-turn coil	10-turn coil
Case I: $\boldsymbol{V}_p$ (4 dimensions)	MOD: 93.54% Error in x: 1.51 mm Error in y: 1.60 mm Error in z: 1.47 mm	MOD: 80.9% Error in x: 6.75 mm Error in y: 7.14 mm Error in z: 3.45 mm
Case II: $\{\boldsymbol{V}_{in}, \boldsymbol{V}_p\}$ (6 dimensions)	MOD: 92.13% Error in x: 0.93 mm Error in y: 0.96 mm Error in z: 0.73 mm	MOD: 84.39% Error in x: 1.00 mm Error in y: 1.07 mm Error in z: 0.69 mm

C. *Misalignment and clearance variance prediction*

In some scenarios, as in the case of WPT for factory robots,

there is little possibility of the existence of foreign metal objects in the WPT system. In such a case, the user would be interested only in misalignment and clearance variance prediction because it affects the transfer efficiency. For this reason, we trained and evaluated NNs only for the position prediction using the training data without metal objects. The hyperparameters and structure of the NN remained unchanged, except for setting the weight of loss of MOD to 0 to build an NN specialized in the position prediction.

The results are summarized in Table III. Compared to the NN mentioned in the previous section, it has higher accuracy in the prediction of misalignment distances and clearance variance, especially when the combined data $\{\boldsymbol{V}_{in}, \boldsymbol{V}_p\}$ are used for the input data to the NN.

Fig. 7 shows the dependence of the error in the position prediction on the number of cases when using $\{\boldsymbol{V}_{in}, \boldsymbol{V}_p\}$. The accuracy depends on the number of turns. For the 15-turn model, the error can be reduced to 0.5 mm by increasing the number of training data cases.

D. Effect of noise

To know the effect of noise in the data on the performance of the trained NN, we added random noise to the original data. The noise level was mapped to the equivalent size variation in the foreign metal object, both of which cause the same change in the input and differential voltages. We considered the two different noise levels which are equivalent to the size variation ranging from 32 to 35 mm for the input voltage and 30 to 35 mm for the differential voltage in Case A, and the size ranging from 25 to 35 mm for the input voltage and 20 to 35 mm for the differential voltage in Case B. It is assumed that there is no misalignment and the metal object is placed at a certain position. The results are summarized in Table VI. It can be seen that there is no significant differences in the accuracy of MOD, while that of the misalignment prediction clearly becomes worse with the noise level. However, the latter error is still lower than 4 mm. The prediction accuracy depends on the noise level in the real environment, which should be measured for the design of this detection system.

TABLE III
MOD ACCURACY AND ERROR IN POSITION PREDICTION OF THE TRAINED NN (WITHOUT MOD)

	15-turn coil	10-turn coil
Case I: $\boldsymbol{V}_p$ (4 dimensions)	Error in x: 1.07 mm Error in y: 1.17 mm Error in z: 1.21 mm	Error in x: 6.69 mm Error in y: 6.41 mm Error in z: 3.24 mm
Case II: $\{\boldsymbol{V}_{in}, \boldsymbol{V}_p\}$ (6 dimensions)	Error in x: 0.46 mm Error in y: 0.40 mm Error in z: 0.34 mm	Error in x: 0.74 mm Error in y: 0.88 mm Error in z: 0.53 mm

TABLE IV
ACCURACY FOR MOD AND POSITION PREDICTION UNDER NOISY ENVIRONMENT (15TURNS)

	Original data	Case A	Case B
MOD	92.13%	88.9%	94.1 %
Error in x	0.93 mm	2.07 mm	3.51 mm
Error in y	0.96 mm	2.13 mm	3.76 mm
Error in z	0.73 mm	1.60 mm	2.21 mm

V. CONCLUSION

We proposed a new method that realizes MOD together with the prediction of misalignment distances for WPT systems consisting of magnetic cores. We performed approximately 1500 field computations for different misalignment distances in three directions and a metal object with a random position to build the training data for the NN. Using the differential voltages of the detection coils and input voltage of the primary coil as input vectors, we trained the NN to predict the existence of a metal object and the misalignment distance between the two transmitting coils at the same time. In the best case, the trained NN has an accuracy of over 90% for MOD, and the mean absolute error in the misalignment distance is less than 1 mm. By training the NN to predict only the misalignment distance, the error can be reduced to 0.5 mm at best.

ACKNOWLEDGMENT

This work was supported by the MEXT D-DRIVE-HU program and JST SPRING Grant Number JPMJSP2119.

REFERENCES

[1] X. Liu, S. Y. Hui, "Optimal design of a hybrid winding structure for planar contactless battery charging platform," *IEEE Trans. Power Electronics*, vol. 23, no. 1, pp. 455-463, 2008.

[2] M. Budhia, J. Boys, G. Covic, C. Huang. "Development of a single-sided flux magnetic coupler for electric vehicle IPT charging systems." *IEEE Transactions on Industrial Electronics*, vol. 60, no. 1, pp. 318-328, 2013.

[3] Y. Gong, Y. Otomo, H. Igarashi, "Multi-objective topology optimization of magnetic couplers for wireless power transfer," *International Journal of Applied Electromagnetics and Mechanics*, vol. 64, no. 1-4, pp. 325-333 2020.

[4] International Commission on Non-Ionizing Radiation Protection, "Guidelines for limiting exposure to time-varying electric and magnetic fields (1 Hz to 100 kHz)," *Health Phys.*, vol. 99, no. 6, pp. 818–836, 2010.

[5] V. Thai, J. Park, S. Jeong, C. Rim, Y. Kim, "Equivalent-circuit-based design of symmetric sensing coil for self-inductance-based metal object detection," *IEEE Access*, vol. 8, pp. 94190-94203, 2020.

[6] L. Xiang, et al, "Foreign object detection in a wireless power transfer system using symmetrical coil sets," *IEEE Access*, vol. 7, pp. 44622-44631, 2019.

[7] Y. Gong, Y. Otomo, H. Igarashi, "Sensorless metal object detection for wireless power transfer using machine learning," *COMPEL-The international journal for computation and mathematics in electrical and electronic engineering*, Vol .41, No. 3, pp. 807-823, 2021.

[8] M. Ote, S. Jeong, M. Tentzeris, "Foreign object detection for wireless power transfer based on machine learning," *2020 IEEE Wireless Power Transfer Conference* (WPTC), 2020.

[9] K. Jung, J. Park, S. Son and S. Ahn, "Position prediction of wireless charging electric vehicle for auto parking using extreme gradient boost algorithm," *2020 IEEE Wireless Power Transfer Conference* (WPTC), 2020.

[10] S. Son et al., "Foreign object detection of wireless power transfer system using sensor coil," *2021 IEEE Wireless Power Transfer Conference* (WPTC), 2021.

[11] B. Mickel, G. A. Covic, and J. T. Boys, "Design and optimization of circular magnetic structures for lumped inductive power transfer systems," *IEEE Transactions on Power Electronics*, vol. 26, no. 11, pp. 3096-3108, 2011.

[12] Electric vehicle wireless power transfer (WPT) systems - Part 3: Specific requirements for the magnetic field wireless power transfer systems, 2019

[13] M. Abadi, P. Barham, J. Chen, et al, "Tensorflow: A system for large-scale machine learning," *12th USENIX symposium on operating systems design and implementation*, 265-283, 2016.

[14] F. Pedregosa et al., "Scikit-learn: Machine learning in Python," *the Journal of Machine Learning research 12*, 2825-2830, 2011.